

Improving Photocatalytic Efficiency with Titanium Dioxide Quantum Dots

Nam Duy Dao¹, Tho Thi Lam², Anh Dieu Van¹, Ha Thi Thu Vu², Hai Trung Huynh^{3,*}

¹School of Chemistry and Life Science, Hanoi University of Science and Technology, 1 Dai Co Viet Road, Hai Ba Trung, Hanoi, Vietnam.

²National Key Laboratory for Petrochemical and Refinery Technology, 2 Pham Ngu Lao Street, Hoan Kiem District, Hanoi, Vietnam.

³School of Materials Science and Engineering, Hanoi University of Science and Technology, 1 Dai Co Viet Road, Hai Ba Trung, Hanoi, Vietnam.

Received: 26th June 2024; Revised: 3rd August 2024; Accepted: 4th August 2024
Available online: 25th August 2024; Published regularly: October 2024



Abstract

Titanium dioxide quantum dots (TiO₂-QDs), synthesized using a microwave-assisted method, represent a significant advancement in photocatalysis, particularly in the treatment of environmental pollutants. This study focuses on TiO₂-QDs synthesized at 200°C for a duration of 5 minutes, using titanium butoxide as a precursor. Characterization through TEM, XRD, PL, and UV-Vis-DRS analyses revealed uniform quantum dots with an average size of 5.28 nm, a bandgap energy of 3.22 eV, and a crystalline anatase phase, indicative of high photocatalytic activity. Notably, these TiO₂-QDs demonstrated exceptional performance in degrading methylene blue (MB) in water, achieving a remarkable treatment efficiency of 97.6% in 120 min, significantly outperforming both conventional titanium dioxide nanoparticles and commercial titanium dioxide materials. The reaction conditions were evaluated based on factors such as catalyst dose, initial MB concentration, and pH. The results indicate that optimal degradation efficiency of MB was achieved at a pH of 7, with a catalyst dose of 0.15 g/L and at a low MB concentration. The efficiency slightly decreased to 94.5% after five reuse cycles, emphasizing its significant reusability and stability.

Copyright © 2024 by Authors, Published by BCREC Publishing Group. This is an open access article under the CC BY-SA License (<https://creativecommons.org/licenses/by-sa/4.0>).

Keywords: TiO₂ quantum dot; TiO₂ photocatalyst; methylene blue treatment; microwave-assisted method

How to Cite: N.D. Dao, T.T. Lam, A.D. Van, H.T.T. Vu, H.T. Huynh (2024). Improving Photocatalytic Efficiency with Titanium Dioxide Quantum Dots. *Bulletin of Chemical Reaction Engineering & Catalysis*, 19 (3), 408-417 (doi: 10.9767/bcrec.20176)

Permalink/DOI: <https://doi.org/10.9767/bcrec.20176>

1. Introduction

Titanium dioxide (TiO₂), identified as a semiconductor by researchers Fujishima and Honda in 1972 [1], has been a focal point of extensive research for its distinctive properties and broad applications. Recognized for its outstanding photocatalytic activity, chemical stability, non-toxicity, and UV light absorption capabilities [2–4], this naturally occurring titanium oxide serves as an ideal material for various applications in advanced fields like photoptoelectronics, photodetectors, photovoltaics, and photocatalysis [5–8].

The TiO₂ has been extensively researched for its application in treating pollutants in water environments, demonstrating high efficiency in the degradation of organic compounds such as dyes, pharmaceuticals, and pesticides, as well as inorganic compounds like metals and nitrates. The drive to enhance TiO₂'s photocatalytic efficiency is not just about improving water treatment capabilities; it's also about advancing environmental sustainability, reducing reliance on non-renewable resources [9–14].

The photocatalytic efficiency of TiO₂ is significantly influenced by several factors, including its specific surface area, crystal phase, crystallite size, crystallinity, and the presence of dopants. Consequently, research efforts have been

* Corresponding Author.
Email: hai.huynhtrung@hust.edu.vn (H.T. Huynh)

dedicated to enhancing this efficiency by increasing the surface area and porosity through the fabrication of various structures, such as nanoparticles, nanowires, nanorods, nanosheets, mesoporous spheres, nanobelts, nanotubes, and urchin-like clusters [15]. Additionally, chemical modifications involving the doping with non-metals (nitrogen, F, C, S), noble metals (Ag, Au, Pt, and Pd), or other metals (Cr, Co, V, Fe, etc.) are explored to reduce the bandgap energy and minimize electron-hole recombination [3,16–20].

In recent years, TiO₂ quantum dot materials have garnered interest as highly potential materials with outstanding properties that enhance catalytic activity [21]. Quantum dots are nearly quasi-zero-dimensional nanostructures composed of a small number of atoms, typically ranging in size from about 2-10 nm [22–23]. These sizes are smaller than or roughly equal to the Bohr radius of an exciton in three-dimensional space, and they are small enough to exhibit quantum mechanical properties [21]. "Small" in this context is defined in relation to the characteristic size of the electron-hole pair (exciton) binding in semiconductor materials. As a result, the photocatalytic properties are enhanced, making better use of the stimulating photon energy and reducing electron recombination [21,22,24]. Unlike nano sized TiO₂ particles, TiO₂ quantum dots have small and uniform particle sizes, do not aggregate, exhibit high photocatalytic activity, and maintain high stability while being reusable [25].

Published studies have focused on sol-gel methods using precursors, such as titanium isopropoxide, titanium butoxide, and inorganic salts like titanium tetrachloride as well as hydrothermal methods using precursors like titanium (IV) bis(ammonium lactate)dihydroxide (TiBALDH) and titanium oxychloride (TiOCl₂), or inorganic salt Ti(SO₄)₂. These methods have yielded relatively uniform particle sizes with size distributions ranging from 2.5 to 7 nm, with only Shim *et al.* achieving an average size of 15 nm [24–32]. Most materials obtained from these studies have lower bandgap energies than that of anatase materials, typically around 3.2 eV, although some materials have very large bandgaps, as seen in Rehan Danish *et al.*, 2014 research, reaching as high as 4.35 eV, which can limit the visible light absorption [25,31–32].

In this study, TiO₂ quantum dots were synthesized using a microwave-assisted method. This method utilized a microwave oven, taking 10 min to reach a temperature of 200 °C and an additional 5 min for the synthesis of the material. This method offers significant benefits, including a reduced synthesis time and lower energy consumption compared to both the sol-gel and hydrothermal methods. Moreover, it features a

more stable and controllable synthesis process. Its cost-effectiveness and high product efficiency also make it suitable for industrial-scale [25,29]. These quantum dots underwent detailed characterization to assess their size, shape, crystallinity and essential structural properties. Furthermore, their photocatalytic performance and stability were tested in degradation of methylene blue in water, a standard organic compound in photocatalysis studies. This test aimed to evaluate not only the quantum dot capacity for degrading organic pollutants but also their durability in practical applications.

2. Materials and Methods

2.1 Materials

In this study, the following reagents were employed: titanium butoxide (97%) (TBOT), isopropyl alcohol (IPA) (≥99%), ethanol (EtOH) (≥99%), and methylene blue, all sourced from Sigma-Aldrich. Titanium dioxide nanoparticles (TiO₂-NP, TiO₂ 99.9%, APS 25 nm) were acquired from Degussa, while commercial titanium dioxide (TiO₂-CM, 99% purity) was purchased from Xilong. An aqueous MB solution of 10 ppm was used as the model reagent in the photocatalytic experiments. Deionized water (DI) used in all experiments (18 MΩ cm⁻¹ in resistivity) was produced in the laboratory.

2.2 Synthesis of Titanium Dioxide Quantum Dot

The synthesis of TiO₂-QDs using the microwave-assisted method as follows: initially, 10 mL of IPA was slowly added to 10 mL of TBOT, and the mixture was continuously stirred for 15 min to obtain solution A. Next, solution A was slowly added to 100 mL of deionized water (DI) in a 250 mL beaker, and the mixture was continuously stirred for 1 h to form solution B. The entire solution B was transferred to two 100 mL teflon containers and placed in a microwave device. The reaction was carried out in a microwave oven with the following settings: preheating time of 10 min from room temperature to 200 °C, followed by a 5-min reaction at 200 °C, and then cooled to room temperature. The catalyst was then recovered by centrifugation at a speed of 5500 rpm. The catalyst was washed with EtOH at least three times to remove any residual products and then dried at 70 °C.

The resulting solid product was finely ground and calcined in an air environment at 450 °C for 2 h, with a heating rate of 5 °C per min. The material was then naturally cooled to room temperature to enhance the crystallization process, achieve uniform and stable crystal sizes, and improve the photocatalytic activity. Finally, the product was ground again.

2.3 Characterizations

TiO₂ quantum dots were characterized for their crystalline phase composition and structures by X-ray diffraction (XRD) measurements using a PANalytical X'Pert PRO instrument. Surface morphology and material size were assessed using a Transmission Electron Microscope (TEM) (Philips Tecnai 10 Microscope) operating at 200 kV. Surface morphology, structure, and composition were analyzed using Scanning Electron Microscopy (SEM), and Energy Dispersive X-ray (EDX) techniques with a TM4000Plus tabletop Microscope (HITACHI). The UV-Vis diffused reflectance spectroscopy (UV-Vis-DR) of the samples was measured using a JASCO V-750 spectrophotometer. Photoluminescence of the samples was recorded using an iHR 550 Horiba instrument. Raman spectroscopy was performed using a Renishaw in Via Raman system with a 514 nm laser.

2.4 Photocatalytic Tests

The investigation of photocatalytic activity and material durability was conducted by comparing three samples: TiO₂-QDs, TiO₂ NPs and commercial TiO₂ CM. The selected solution for treatment was methylene blue, which is a polycyclic aromatic compound commonly used as a representative model for experiments involving the degradation of Persistent Organic Pollutants. The experiment was carried out using a high-pressure mercury lamp OSRAM 150W as the white light source, and the light intensity was measured using an advanced light meter from Geneq with the result showing the photoluminescence intensity of 5.0 mW.cm⁻². Methylene blue solution was placed in a double-walled glass beaker, which was temperature-controlled using a heating system to maintain a constant temperature of 25 °C throughout the

reaction. The photocatalytic activity testing apparatus was placed inside a sealed chamber, equipped with a stirring device to ensure uniform mixing and enhance treatment efficiency. Inside the system, there was also an exhaust fan to ensure proper air circulation within the entire system.

The general experimental procedure is as follows: Prepare 0.1 g of catalyst (TiO₂-QDs, TiO₂ NPs, TiO₂ TM) and add it to 400 mL of MB solution with a concentration of 10 ppm. The mixture is stirred in the dark condition until adsorption/desorption equilibrium condition. Subsequently, the solution was introduced into the photoreactor for the extended light irradiation experiment. According to the sampling schedule, catalyst samples were centrifuged using a centrifuge device (Centrifuge model DSC158T, Taiwan), and the MB concentration was determined through UV-Vis Spectrophotometer (model UV-2600, Shimadzu, Japan) at a wavelength of 663 nm. Photocatalytic degradation was assessed based on C_t/C_0 vs. time, where C_0 and C_t represent the MB concentrations in the solution before irradiation ($t = 0$) and after irradiation for t minutes, respectively.

The photocatalytic degradation efficiency of MB was calculated as followed:

$$\eta\% = \frac{C_0 - C_t}{C_0} \times 100 \quad (1)$$

The reusability test incorporated a procedure in which the catalyst material was collected after each photocatalytic degradation experiment. Each experimental cycle included 120 min of irradiation, following which the materials were isolated from the mixture using filtration and centrifugation processes. To prepare them for the next cycle, these materials were then dried at a temperature of 100 °C.

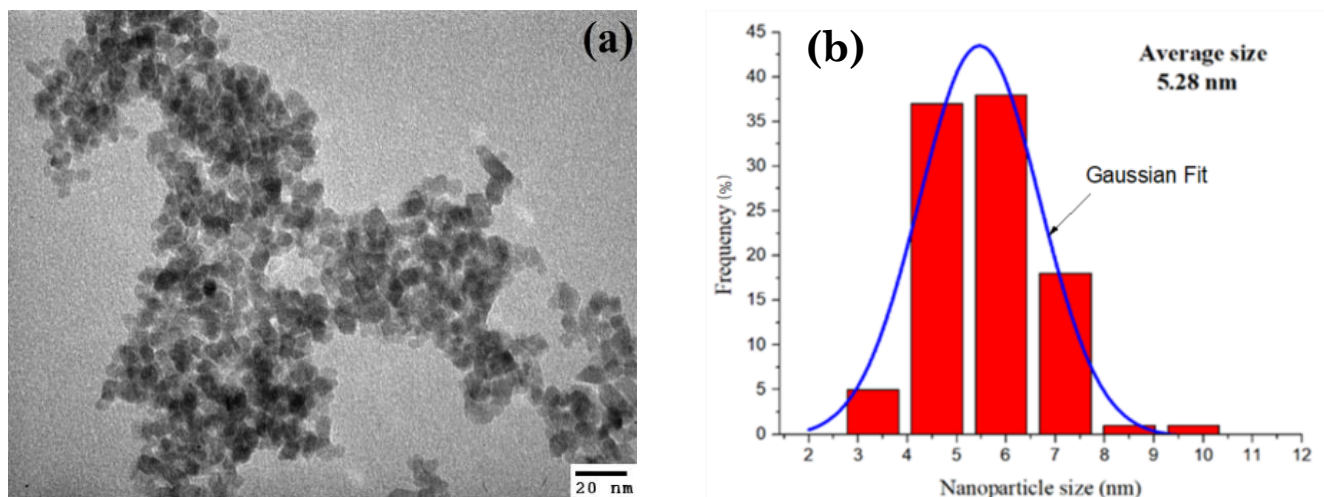


Figure 1. TEM image (a) and (b) Particle size distribution of TiO₂-QDs.

3. Results and Discussion

3.1 Characterizations of Material

The surface structure of TiO₂ material through TEM imaging results is presented in Figure 1. The Transmission electron microscopy (TEM) image in Figure 1 illustrates the uniform spherical particles in the TiO₂-QDs material. The material was synthesized using a microwave method, with particle sizes ranging from 3.1 to 10 nm, with the main distribution occurring in the range of 4-7 nm. The average value of the TiO₂-QDs sample size was found to be 5.28 nm.

The fluorescence spectrum of the TiO₂-QDs is shown in Figure 2. Fluorescence emission was observed in the range of 400-800 nm when excited with light at a wavelength of 360 nm. The results indicate that in the fluorescence spectrum of TiO₂-QDs synthesized using the microwave-assisted method, there is a peak maximum at approximately 525 nm. Here, the peak at 525 nm is attributed to the indirect recombination of the photogenerated electrons and holes via the oxygen vacancies [33]. Additionally, indirect recombination at the 525 nm peak is noticeable in the TiO₂-QDs sample with a fairly distinct peak.

To investigate the absorption properties and band structure of the obtained TiO₂-QDs, UV-Vis diffuse reflectance spectroscopy (UV-Vis DRS) was conducted alongside the TiO₂ NPs sample. The results, shown in Figure 3(a), reveal that the absorption edge of the microwave-synthesized sample has a narrower bandgap compared to the TiO₂ NPs sample. UV-Vis DRS spectral analysis not only provides information about the absorption regions of the catalyst materials but also allows for the calculation of the bandgap energy (E_g). The bandgap energy was calculated using the Tauc plot of $(Ah\nu)^{1/2}$ versus wavelength $h\nu$. The results are presented in Figure 3(b). The

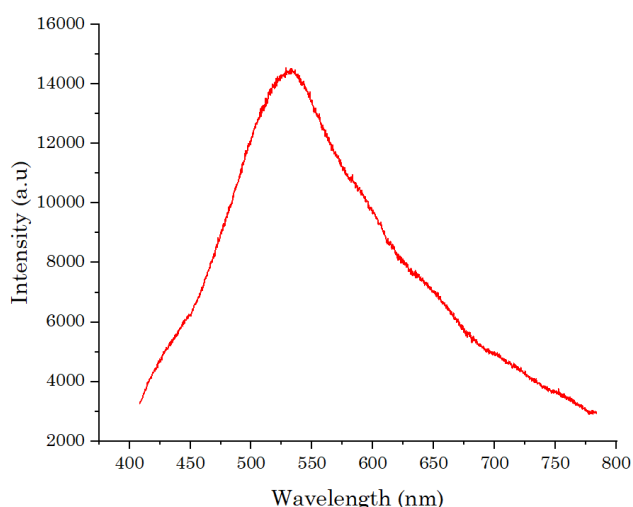


Figure 2. Photoluminescence (PL) spectra of TiO₂-QDs.

calculated bandgap energy of TiO₂-QDs is 3.22 eV, which is higher than that of TiO₂ CM at 2.98 eV and TiO₂ NPs at 2.95 eV. This higher bandgap enhances their photocatalytic activity due to the quantum confinement effect, which reduces electron-hole recombination. The increased bandgap allows TiO₂-QDs to utilize UV light more effectively, making them crucial for photocatalytic applications.

The increase in bandgap energy of the microwave sample can be explained by the Brus model, specifically that when the TiO₂ particle size is less than 10 nm, the bandgap energy increases slightly as the particle size decreases [34]. In addition, factors affecting the bandgap energy include the crystal phase of the material, as well as the synthesis method and conditions such as temperature and atmosphere [35–36].

The crystal structure of TiO₂ quantum dots (QDs) was studied using X-ray diffraction (XRD), as shown in Figure 4. The XRD pattern reveals the presence of distinct diffraction peaks at 25.40°, 37.2°, 38.50°, 37.2°, 48.20°, 54.2°, 55.1°, and 55.1°.

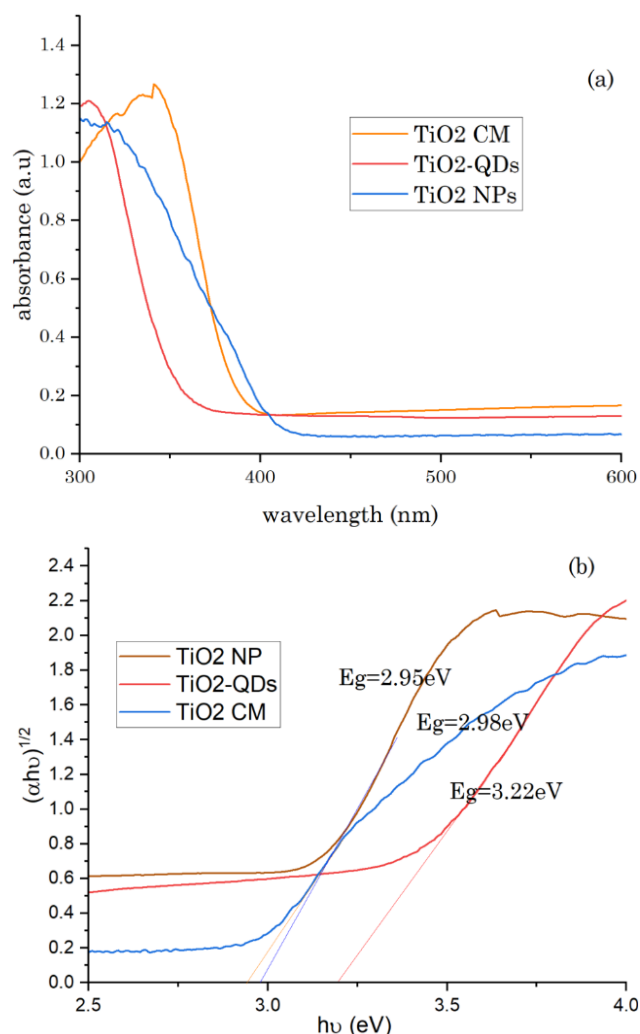


Figure 3. UV-Vis (a) and bandgap (b) of TiO₂-QDs and TiO₂ NPs.

62.8°, 68.9°, 70.4°, and 75.3° (2 θ) corresponding to crystal lattice planes (101), (103), (004), (112), (200), (105), (211), (204), (116), (220), and (215), respectively. These peaks are characteristic of the crystalline phase structure of anatase, corroborating previous XRD studies on TiO₂ anatase phase samples [23,27,33]. Furthermore, Figure 4 demonstrates the absence of any characteristic peaks for the rutile phase or any other crystalline phases. Calculate the average particle size using XRD analysis results, employing the Scherrer equation for the most intense (101) diffraction peak. The calculated average size, $D = 5.83$ nm, closely aligns with the value obtained via the TEM method. The anatase phase of TiO₂ is recognized for its superior photocatalytic capabilities, attributed to its higher electron mobility compared to the rutile phase. This property significantly enhances the efficiency of pollutant degradation under UV light.

The chemical composition of the TiO₂-QDs sample was analyzed using Energy Dispersive X-ray (EDX) spectroscopy (Figure 5), which indicated that the TiO₂-QDs sample contains only titanium and oxygen without any other impurities. Raman spectroscopy provides valuable information about the purity and crystallinity of a phase and is a powerful tool in

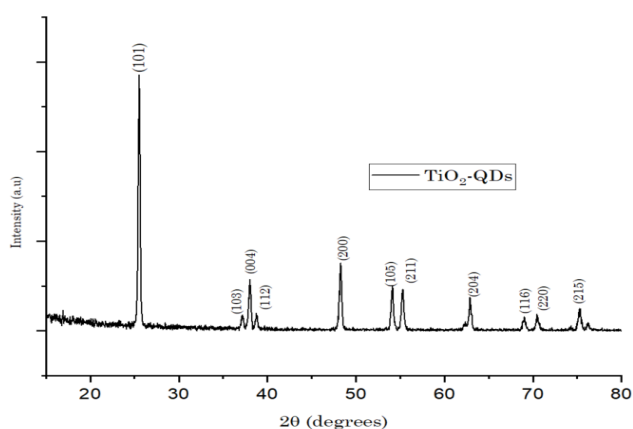


Figure 4. XRD pattern of TiO₂-QDs synthesized.

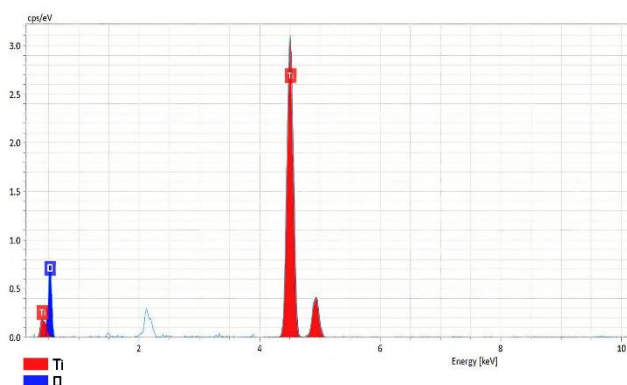


Figure 5. EDX spectrum of TiO₂ quantum dot.

the study of heterogeneous catalyst materials. Figure 6 presents the Raman spectrum in the range of 100-800 cm⁻¹ for the TiO₂-QDs sample. Peaks at approximately 152, 195, 402, 520, and 645 cm⁻¹ are assigned to the anatase phase of TiO₂ (space group D194h). These peaks correspond to five Raman-active modes with respective symmetries: $E_g(1)$, $E_g(2)$, B_{1g} , $A_{1g} + B_{1g}(2)$, and $E_g(3)$ [38]. These results corroborate the consistency between the XRD and Raman spectra.

3.2 Photocatalytic Activity

3.2.1 Investigate of the photocatalytic activity of TiO₂ catalysts

The photocatalytic activity of TiO₂ materials was evaluated under the same optimal conditions, including the following parameters. Prior to irradiation, the catalyst was introduced into the methylene blue (MB) solution and continuously stirred in darkness to assess the adsorption-desorption equilibrium. Observations indicated that equilibrium was reached 30 min after the addition of the catalyst, with no further changes noted upon extending the duration to 60 min. This suggests that the adsorption-desorption equilibrium was established within the first 30 min.

UV-Vis results confirmed that the photocatalytic activity of the synthesized TiO₂ materials could be assessed using UV light due to the wide bandgap of TiO₂-QDs, which is 3.22 eV. The photodegradation efficiency of methylene blue by commercial TiO₂, TiO₂-NPs, and TiO₂-QDs catalysts is presented in Figure 7(a). The results indicate that under the same experimental conditions, the degradation of methylene blue using the microwave-synthesized sample is significantly higher than that of the two

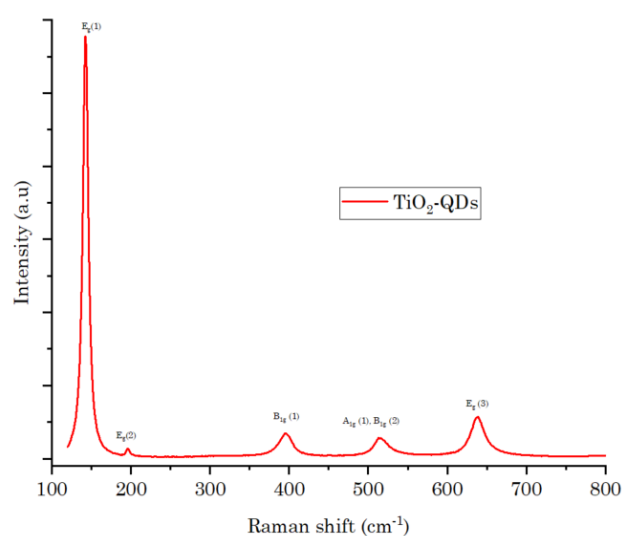


Figure 6. Raman Shift spectrum of TiO₂-QDs sample.

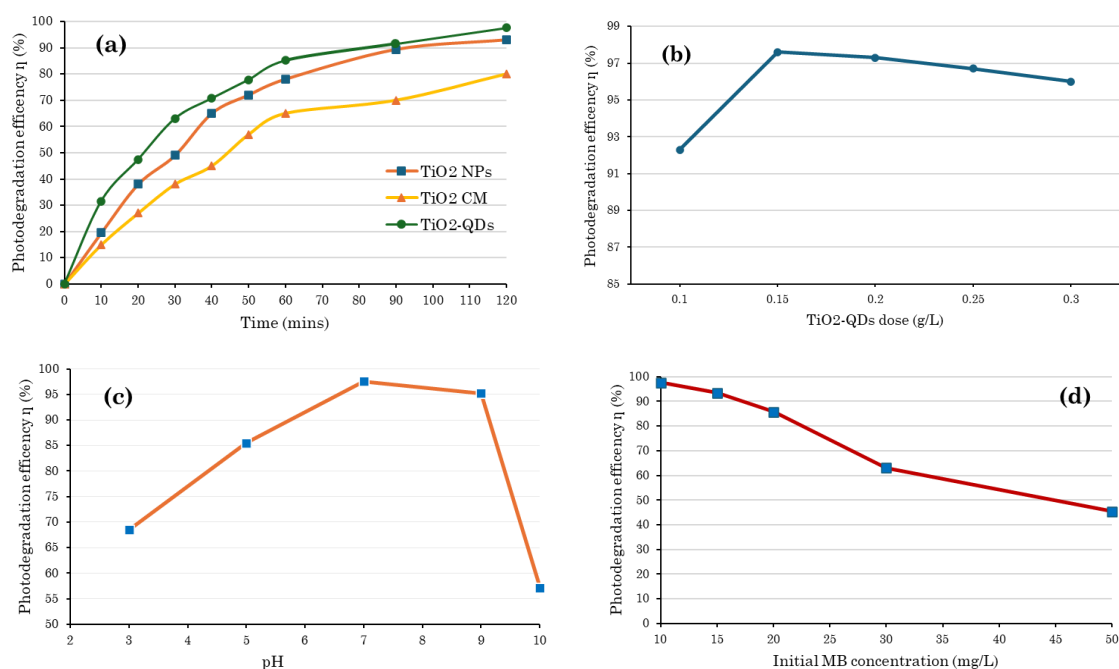


Figure 7. Photodegradation efficiency of methylene blue by (a) different TiO₂ catalyst, (b) TiO₂-QDs dose, (c) pH and (d) initial MB concentration.

Table 1. Comparison between this work and other already published. (ND: Not defined)

No	Precursor	Sample	Method	Bandgap (eV)	Treatment	% of degradation	References
1	Ti(OBu) ₄	TiO ₂ -QDs	Microwave-assistant	3.22	MB	97.6	This study
2	-	TiO ₂ CM	Commercial	ND	MB	80	This study
3	-	TiO ₂ NPs	P25-Degussa	2.95	MB	93	This study
4	TTIP	TiO ₂ /HTC4	hydrothermal	ND	MB	91.9	[39]
5	ZAD	ZnO	Sol-gel	3.48	MB	99	[40]
6	ZAD	ZnO	Precipitation	3.31	MB	98	[40]
7	ZAD	ZnO	Thermal decomposition	3.27	MB	85	[40]
8	Zn(NO ₃) ₂ ·6H ₂ O	ZnO/N-CQD	hydrothermal	3.129	MB	80% Higher ZnO (after 30 mins)	[41]
9	TTIP	TiO ₂ QDs	Sol-gel	3.79	MB	97.9	[27]
10	TTIP	TiO ₂ QDs	Sol-gel	3.76	ND	ND	[25]
11	TiCl ₄	TiO ₂ QDs	Sol-gel	2.85	MO	Higher TiO ₂ -P25	[26]
12	Ti(OBu) ₄	TiO ₂ QDs	Sol-gel	ND	Indigo Carmine dye	100%	[24]
13	TTIP	TiO ₂ QDs	hydrothermal	3.51	ND	-	[28]
14	TiBALDH and TiOCl ₂	TiO ₂ QDs	hydrothermal	ND	RhB and MO	100%, higher TiO ₂ -P25	[29]
15	Ti(SO ₄) ₂	TiO ₂ QDs	hydrothermal	3.38, 3.47, 3.25	ND	ND	[30]
16	Ti(OBu) ₄	TiO ₂ QDs	Microwave-assistant	3.69, 3.93, 3.99, 4.35	ND	ND	[31]

commercial TiO₂ samples, TiO₂ NPs. Specifically, after 90 min of irradiation, the degradation efficiency of MB for TiO₂-QDs, TiO₂ NPs, and TiO₂ CM were 97.6%, 93%, and 80%, respectively.

Figure 7(a) shows that as the irradiation time increases, the photocatalytic degradation efficiency of MB also increases, indicating complete degradation of the dye. After 120 min of irradiation, the degradation of the model reaction MB is almost complete for the microwave-synthesized TiO₂-QDs sample, reaching 97.6%. It is evident that TiO₂-QDs have exhibited superior photocatalytic degradation compared to nano-sized TiO₂ particle catalysts and commercial TiO₂. The difference in the degradation time of MB depends on the synthesis method, size, and morphology of the obtained materials. Indeed, the improved photocatalytic activity of TiO₂-QDs can be attributed to their quantum properties, such as ultra-small particle size, and enhanced charge carrier separation. These results are consistent with previous publications [25–27].

Table 1 presents several studies on the synthesis of materials and their ability to treat organic compounds in water using photocatalytic materials. These studies demonstrate that self-synthesized quantum dot TiO₂ is effective in treating organic compounds and often outperforms TiO₂ nanoparticles (P25-Degussa). Additionally, comparing the photocatalytic activity and stability of different synthesized materials is challenging due to the many factors that influence the photocatalytic process [42]. Within the scope of this study, TiO₂ quantum dots exhibit superior methylene blue (MB) degradation efficiency compared to TiO₂ nanoparticles and TiO₂ commercial material.

3.2.2 Investigating the factors affecting the efficiency of catalysts

The study of factors influencing the photocatalytic efficiency of TiO₂-QDs for MB treatment involved sequentially altering variables including catalyst concentration, pH, and initial concentration of MB to identify optimal parameters. The investigation was conducted by adjusting one parameter at a time while keeping the others constant and irradiation time 120 minutes.

The investigation of TiO₂-QDs concentration ranging from 0.1 to 0.3 g/L, as shown in Figure 7(b), indicates that the degradation efficiency gradually increases from a concentration of 0.1 g/L, reaches optimum concentration at 0.15 g/L, and subsequently decreases as the concentration reaches 0.3 g/L. This pattern suggests that increasing concentration leads to a higher density of active sites on the catalyst, thus enhancing the degradation efficiency of MB. However, beyond a certain point, the excessive TiO₂ particles obstruct

photons from reaching some of the catalyst particles, resulting in a reduction of the treatment efficiency [43].

The results of the pH influence on the solution, shown in Figure 7(c), demonstrate that with values ranging from 3 to 10, the efficiency increases as the pH rises, reaching a maximum at pH 7 and then gradually decreases up to pH 10. This trend is understandable given that the point of zero charge (pH_{pzc}) is reported to be approximately 6.8 [44]. Therefore, changes in pH affect the adsorption capability of MB on TiO₂-QDs material, consistent with findings from prior research [43–45]. The investigation was conducted with initial MB concentrations from 10 to 50 mg/L. As depicted in Figure 7(d), the degradation efficiency of MB decreases with increasing concentration. This is expected as a higher MB concentration leads to increased MB adsorption on the catalyst surface, thereby hindering the reaction between MB and both the holes and hydroxyl radicals. Additionally, an increase in MB concentration affects the proton absorption efficiency of TiO₂-QDs, resulting in a reduced treatment efficacy as the MB quantity increases [43].

3.2.3 Research on the catalyst's reusability

For industrial and environmental applications, the catalyst's reusability is crucial to determine its long-term stability and potential for reuse. To assess this important parameter, a long-term stability experiment was conducted over 5 consecutive photocatalytic cycles, as depicted in Figure 8. The catalyst materials were exposed to light for 120 min. Following each cycle, the materials were separated using filtration and centrifugation, and subsequently dried at 100 °C.

It can be observed that after all cycles, the photocatalytic activity of the catalyst materials tested was lower than in the first cycle. Notably, after 5 reuse cycles, the photodegradation efficiency of MB decreased from 97.6% to 94.5% for

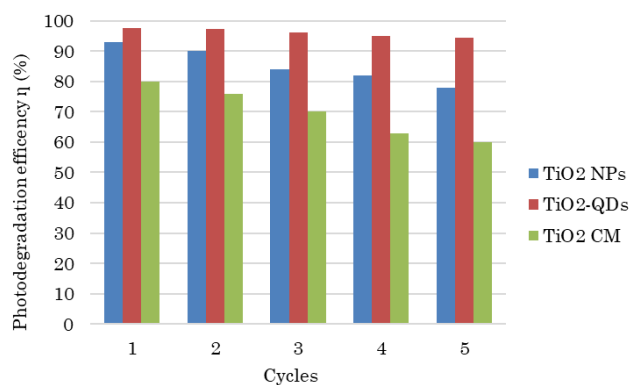


Figure 8. Reusability of commercial TiO₂ catalyst and synthesized nano TiO₂ catalysts.

the TiO₂-QDs, from 93% to 78% for TiO₂ NPs, and from 80% to 60% for the TiO₂ CM. These results indicate that the synthesized TiO₂-QDs catalyst material exhibited better stability and reusability compared to TiO₂ NPs catalysts and commercial TiO₂ CM. Indeed, the photocatalytic activity of TiO₂-QDs only showed a slight decrease, while the rate of decline in the photodegradation efficiency of TiO₂ NPs and commercial TiO₂ was much faster. The decrease in photocatalytic efficiency after repeated cycles can be due to catalyst deactivation from by-product accumulation, physical loss of material, and structural changes like phase shift or agglomeration [46].

4. Conclusion

The study successfully synthesized TiO₂-anatase quantum dot material using a microwave-assisted method, yielding particles predominantly in the range of 4-7 nm. Detailed analysis verified the high purity and crystallinity of the material, significantly devoid of impurities. The synthesized TiO₂-QDs exhibited superior photocatalytic activity and durability compared to commercial TiO₂ counterparts, evidenced by an impressive MB degradation with efficiency of 97.6% for methylene blue in 120 min of irradiation. The efficiency slightly reduced to 94.5% after five cycles, highlighting the durability and reusability of TiO₂-QDs. The investigation of reaction conditions reveals that the highest MB degradation efficiency was achieved with a pH of 7, a catalyst dose of 0.15 g/L, and a low concentration of MB. These findings highlight the potential of TiO₂-QDs as a highly effective and stable photocatalyst in environmental applications, offering a promising direction for future research and development in this field.

Acknowledgement

This work was supported by the Ministry of Science and Technology, Vietnam under grant number ĐTDL.CN-67/19.

CRedit Author Statement

T.H Thi Vu supervised, conceptualized and planned the work, conceived and designed photocatalyst synthesis experiments, and reviewed and edited the manuscript. Dao Duy Nam performed the photocatalysis experiments, analyzed and interpreted the data, and wrote and edited the manuscript. Trung Hai Huynh supervised, came up with ideas and planned the work. Tho Thi Lam performed photocatalyst synthesis experiments and collected data. Dieu Anh Van performed experiments testing catalysts. All authors discussed the results and commented on the manuscript.

Declaration of Competing Interest

We certify that this manuscript consists of original, unpublished work which is not under consideration for publication elsewhere. We declare no competing financial interest.

References

- [1] Fujishima, A., Honda, K. Electrochemical Photolysis of Water at a Semiconductor Electrode. *Nature*, 238, 37–38 (1972). DOI: 10.1038/238037a0.
- [2] Nakata, K., Fujishima, A. (2012). TiO₂ photocatalysis: Design and applications. *Journal of Photochemistry and Photobiology C: Photochemistry Reviews*, 13(3), 169–189. DOI: 10.1016/j.jphotochemrev.2012.06.001.
- [3] Xiu, Z., Xiu, Z., Guo, M., Zhao, T., Pan, K., Xing, Z., Li, Z., Zhou, W. (2022). Recent advances in Ti³⁺ self-doped nanostructured TiO₂ visible light photocatalysts for environmental and energy applications. *Chemical Engineering Journal*, 382, 123011. DOI: 10.1016/j.cej.2019.123011.
- [4] Li, Z., Wang, S., Wu, J., Zhou, W. (2022). Recent progress in defective TiO₂ photocatalysts for energy and environmental applications. *Renewable and Sustainable Energy Reviews*, 156, 111980. DOI: 10.1016/j.rser.2021.111980.
- [5] Zargar, R.A., Arora, M., Bhat, S.A., Mearaj, T., Manthrammel, M.A., Shkir, M. (2023). Growth of TiO₂-CdO coated films: A brief study for optoelectronic applications. *Journal of Physics and Chemistry of Solids*, 179, 111390. DOI: 10.1016/j.jpcs.2023.111390.
- [6] Shaikh, Shoyebmohamad F., Sharifah Mohammed Ali Al-Moayid, Balaji G. Ghule, Mohd Shkir, Haitham Elhosiny Ali, Hamed Majdooa Algarni, Mohd Ubaidullah, and Rajaram S. Mane. "Nanocrystalline and mesoporous anatase TiO₂ films composition and its synthesizing process thereof." *U.S. Patent Application 18/175,920*, filed July 6, 2023
- [7] Herrmann, J.M. (1999). Heterogeneous photocatalysis: Fundamentals and applications to the removal of various types of aqueous pollutants. *Catalysis Today*, 53(1), 115–129. DOI: 10.1016/S0920-5861(99)00107-8.
- [8] Algadi, H., Albargi, H., Umar, A., Shkir, M. (2021). Enhanced photoresponsivity of anatase titanium dioxide (TiO₂)/nitrogen-doped graphene quantum dots (N-GQDs) heterojunction-based photodetector. *Advanced Composites and Hybrid Materials*, 4(4), 1354–1366. DOI: 10.1007/s42114-021-00355-5.
- [9] Rajendran, R., Vignesh, S., Suganthi, S., Raj, V., Kavitha, G., Palanivel, B., Shkir, M., Algarni, H. (2022). g-C₃N₄/TiO₂/CuO S-scheme heterostructure photocatalysts for enhancing organic pollutant degradation. *Journal of Physics and Chemistry of Solids*, 161, 110391. DOI: 10.1016/j.jpcs.2021.110391.

- [10] Gopinath, K.P., Madhav, N.V., Krishnan, A., Malolan, R., Rangarajan, G. (2020). Present applications of titanium dioxide for the photocatalytic removal of pollutants from water: A review. *Journal of Environmental Management*, 270, 110906. DOI: 10.1016/j.jenvman.2020.110906.
- [11] Chen, D., Cheng, Y., Zhou, N., Chen, P., Wang, Y., Li, K., Huo, S., Cheng, P., Peng, P., Zhang, R., Wang, L., Liu, H., Liu, Y., Ruan, R. (2020). Photocatalytic degradation of organic pollutants using TiO₂-based photocatalysts: A review. *Journal of Cleaner Production*, 268, 121725. DOI: 10.1016/j.jclepro.2020.121725.
- [12] Girija, R., Mary, S., Balakrishnan, G., Mariappan, S.M., Hamdy, M.S., Shkir, M. (2022). Noticeably Improved Visible Light Photocatalytic Activity of TiO₂ Nanoparticles through co-Doping of Activated Charcoal and Fe Towards Methylene Blue Degradation. *ChemistrySelect*, 7(5), e202103614. DOI: 10.1002/slct.202103614.
- [13] Vignesh, S., Chandrasekaran, S., Srinivasan, M., Anbarasan, R., Perumalsamy, R., Arumugam, E., Shkir, M., Algarni, H., Al Faify, S. (2022). TiO₂-CeO₂/g-C₃N₄ S-scheme heterostructure composite for enhanced photo-degradation and hydrogen evolution performance with combined experimental and DFT study. *Chemosphere*, 288, 132611. DOI: 10.1016/j.chemosphere.2021.132611.
- [14] Rajendran, R., Vignesh, S., Sasireka, A., Suganthi, S., Raj, V., Baskaran, P., Shkir, M., Al Faify, S. (2021). Designing Ag₂O modified g-C₃N₄/TiO₂ ternary nanocomposites for photocatalytic organic pollutants degradation performance under visible light: Synergistic mechanism insight. *Colloids and Surfaces A: Physicochemical and Engineering Aspects*, 629, 127472. DOI: 10.1016/j.colsurfa.2021.127472.
- [15] Song, L., Jing, W., Chen, J., Zhang, S., Zhu, Y., Xiong, J. (2019). High reusability and durability of carbon-doped TiO₂/carbon nanofibrous film as visible-light-driven photocatalyst. *Journal of Materials Science*, 54(5), 3795–3804. DOI: 10.1007/s10853-018-3105-7.
- [16] Zhu, Y., Xu, T., Zhao, D., Li, F., Liu, W., Wang, B., An, B. (2021). Adsorption and solid-phase photocatalytic degradation of perfluorooctane sulfonate in water using gallium-doped carbon-modified titanate nanotubes. *Chemical Engineering Journal*, 421(P1), 129676. DOI: 10.1016/j.cej.2021.129676.
- [17] Li, Y., Cheng, H., Wang, N., Zhou, S., Xie, D., Li, T. (2019). Annealing effects on the microstructure, magnetism and microwave-absorption properties of Fe/TiO₂ nanocomposites. *Journal of Magnetism and Magnetic Materials*, 471, 346–354. DOI: 10.1016/j.jmmm.2018.09.101.
- [18] Liu, C., Dong, S., Chen, Y. (2019). Enhancement of visible-light-driven photocatalytic activity of carbon plane/g-C₃N₄/TiO₂ nanocomposite by improving heterojunction contact. *Chemical Engineering Journal*, 371, 706–718. DOI: 10.1016/j.cej.2019.04.089.
- [19] Nasralla, N.H.S., Yeganeh, M., Astuti, Y., Piticharoenphun, S., Šiller, L. (2018). Systematic study of electronic properties of Fe-doped TiO₂ nanoparticles by X-ray photoemission spectroscopy. *Journal of Materials Science: Materials in Electronics*, 29(20), 17956–17966. DOI: 10.1007/s10854-018-9911-5.
- [20] Nasralla, N., Yeganeh, M., Astuti, Y., Piticharoenphun, S., Shahtahmasebi, N., Kompany, A., Karimipour, M., Mendis, B.G., Poolton, N.R.J., Šiller, L. (2013). Structural and spectroscopic study of Fe-doped TiO₂ nanoparticles prepared by sol-gel method. *Scientia Iranica*, 20(3), 1018–1022. DOI: 10.1016/j.scient.2013.05.017.
- [21] Sun, P., Xing, Z., Li, Z., Zhou, W. (2023). Recent advances in quantum dots photocatalysts. *Chemical Engineering Journal*, 458, 141399. DOI: 10.1016/j.cej.2023.141399.
- [22] Pandurangan, D.K., Mounika, S.K. (2012). Quantum dot aptamers-an emerging technology with wide scope in pharmacy. *International Journal of Pharmacy and Pharmaceutical Sciences*, 4, 24–31.
- [23] Xue, J., Wang, X., Jeong, J.H., Yan, X. (2020). Fabrication, photoluminescence and applications of quantum dots embedded glass ceramics. *Chemical Engineering Journal*, 383, 123082. DOI: 10.1016/j.cej.2019.123082.
- [24] Sood, S., Kumar, S., Umar, A., Kaur, A., Mehta, S.K., Kansal, S.K. (2015). TiO₂ quantum dots for the photocatalytic degradation of indigo carmine dye. *Journal of Alloys and Compounds*, 650, 193–198. DOI: 10.1016/j.jallcom.2015.07.164.
- [25] Javed, S., Islam, M., Mujahid, M. (2019). Synthesis and characterization of TiO₂ quantum dots by sol gel reflux condensation method. *Ceramics International*, 45(2), 2676–2679. DOI: 10.1016/j.ceramint.2018.10.163.
- [26] Deng, Q., Zhang, W., Lan, T., Xie, J., Xie, W., Liu, Z., Huang, Y., Wei, M. (2018). Anatase TiO₂ Quantum Dots with a Narrow Band Gap of 2.85 eV Based on Surface Hydroxyl Groups Exhibiting Significant Photodegradation Property. *European Journal of Inorganic Chemistry*, 2018(13), 1506–1510. DOI: 10.1002/ejic.201800097.
- [27] Gnanasekaran, L., Hemamalini, R., Ravichandran, K. (2015). Synthesis and characterization of TiO₂ quantum dots for photocatalytic application. *Journal of Saudi Chemical Society*, 19(5), 589–594. DOI: 10.1016/j.jscs.2015.05.002.
- [28] Pandey, S.K., Bhatnagar, A., Shukla, V., Kesarwani, R., Deshpandey, U., Yadav, T.P. (2021). Catalytic mechanism of TiO₂ quantum dots on the de/re-hydrogenation characteristics of magnesium hydride. *International Journal of Hydrogen Energy*, 46(75), 37340–37350. DOI: 10.1016/j.ijhydene.2021.09.006.
- [29] Wu, Z.G., Ren, Z.M., Li, L., Lv, L., Chen, Z. (2020). Hydrothermal synthesis of TiO₂ quantum dots with mixed titanium precursors. *Separation and Purification Technology*, 251, 117328. DOI: 10.1016/j.seppur.2020.117328.

- [30] Shim, Y.J., Choi, G.J. (2016). Characterization of TiO₂ quantum dots synthesized by hydrothermal method. *Transactions on Electrical and Electronic Materials*, 17(2), 125–127. DOI: 10.4313/TEEM.2016.17.2.125.
- [31] Danish, R., Ahmed, F., Koo, B.H. (2014). Rapid synthesis of high surface area anatase Titanium Oxide quantum dots. *Ceramics International*, 40(8), 12675–12680. DOI: 10.1016/j.ceramint.2014.04.115.
- [32] Vu, T.H.T., Lam, T.T., Dao, D.N., Van, D.A., Huynh, T.H. (2023). A Composite of TiO₂ Quantum Dots and TiO₂ Nanoparticles Coated on Anti-Bumping Glass Beads (TiO₂QDs-TiO₂NPs/GBs), with a Very Low Content of TiO₂ as a High Performance Photocatalyst. *Journal of Chemistry*, 2023, 3400175. DOI: 10.1155/2023/3400175.
- [33] Liu, B., Zhao, X., Wen, L. (2006). The structural and photoluminescence studies related to the surface of the TiO₂ sol prepared by wet chemical method. *Materials Science and Engineering: B*, 134(1), 27–31. DOI: 10.1016/j.mseb.2006.06.052.
- [34] Valencia, S., Marín, J.M., Restrepo, G. (2009). Study of the bandgap of synthesized titanium dioxide nanoparticules using the sol-gel method and a hydrothermal treatment. *The Open Materials Science Journal*, 4, 9–14. DOI: 10.2174/1874088X01004010009.
- [35] Danish, R., Ahmed, F., Koo, B.H. (2014). Rapid synthesis of high surface area anatase Titanium Oxide quantum dots. *Ceramics International*, 40(8), 12675–12680. DOI: 10.1016/j.ceramint.2014.04.115.
- [36] Li, Z., Wang, S., Wu, J., Zhou, W. (2022). Recent progress in defective TiO₂ photocatalysts for energy and environmental applications. *Renewable and Sustainable Energy Reviews*, 156, 111980. DOI: 10.1016/j.rser.2021.111980.
- [37] Kaur, A., Umar, A., Kansal, S.K. (2015). Sunlight-driven photocatalytic degradation of non-steroidal anti-inflammatory drug based on TiO₂ quantum dots. *Journal of Colloid and Interface Science*, 459, 257–263. DOI: 10.1016/j.jcis.2015.08.010.
- [38] Martin, M.V., Villabrille, P.I., Rosso, J.A. (2015). The influence of Ce doping of titania on the photodegradation of phenol. *Environmental Science and Pollution Research*, 22(18), 14291–14298. DOI: 10.1007/s11356-015-4667-4.
- [39] Maletić, M., Vukčević, M., Kalijadis, A., Janković-Častvan, I., Dapčević, A., Laušević, Z., Laušević, M. (2019). Hydrothermal synthesis of TiO₂/carbon composites and their application for removal of organic pollutants. *Arabian Journal of Chemistry*, 12(8), 4388–4397. DOI: 10.1016/j.arabj.2016.06.020.
- [40] Saravanan, R., Gupta, V.K., Narayanan, V., Stephen, A. (2013). Comparative study on photocatalytic activity of ZnO prepared by different methods. *Journal of Molecular Liquids*, 181, 133–141. DOI: 10.1016/j.molliq.2013.02.023.
- [41] Widiyandari, H., Prilita, O., Al Ja'farawy, M.S., Nurosyid, F., Arutanti, O., Astuti, Y., Mufti, N. (2023). Nitrogen-doped carbon quantum dots supported zinc oxide (ZnO/N-CQD) nanoflower photocatalyst for methylene blue photodegradation. *Results in Engineering*, 17, 100814. DOI: 10.1016/j.rineng.2022.100814.
- [42] Akpan, U.G., Hameed, B.H. (2009). Parameters affecting the photocatalytic degradation of dyes using TiO₂-based photocatalysts: A review. *Journal of Hazardous Materials*, 170(2–3), 520–529. DOI: 10.1016/j.jhazmat.2009.05.039.
- [43] Abdellah, M.H., Nosier, S.A., El-Shazly, A.H., Mubarak, A.A. (2018). Photocatalytic decolorization of methylene blue using TiO₂/UV system enhanced by air sparging. *Alexandria Engineering Journal*, 57(4), 3727–3735. DOI: 10.1016/j.aej.2018.07.018.
- [44] Salehi, M., Hashemipour, H., Mirzaee, M. (2012). Experimental Study of Influencing Factors and Kinetics in Catalytic Removal of Methylene Blue with TiO₂ Nanopowder. *American Journal of Environmental Engineering*, 2(1), 1–7. DOI: 10.5923/j.ajee.20120201.01.
- [45] Zhang, S., Zhang, J., Sun, J., Tang, Z. (2020). Capillary microphotoreactor packed with TiO₂-coated glass beads: An efficient tool for photocatalytic reaction. *Chemical Engineering and Processing - Process Intensification*, 147, 107746. DOI: 10.1016/j.cep.2019.107746.
- [46] Sonu, K., Puttaiah, S.H., Raghavan, V.S., Gorthi, S.S. (2021). Photocatalytic degradation of MB by TiO₂: studies on recycle and reuse of photocatalyst and treated water for seed germination. *Environmental Science and Pollution Research*, 28(35), 48742–48753. DOI: 10.1007/s11356-021-13863-0.